Charge-changing energy loss, higher-order Z_1 dependence, and pre-equilibrium behavior in the stopping power for energetic ions in solids

N. E. B. Cowern,* P. M. Read, C. J. Sofield, and L. B. Bridwell†
Nuclear Physics Division, Atomic Energy Research Establishment (Harwell), Didcot, Oxon OX11 0RA, United Kingdom

M. W. Lucas
School of Mathematical and Physical Sciences, University of Sussex, Falmer, Brighton, BN1 9QH, Sussex, United Kingdom

(Received 27 December 1983)

Relative stopping cross sections are measured for 3-MeV/u He, Li, and C ions in 2–26-μg/cm^2 C foils. The observed stopping cross sections for the fully stripped He and Li ions scale essentially as Z_1^2, in agreement with standard theory on higher-order Z_1-dependent effects applied to C targets. We observe nonequilibrium charge-state effects in the energy loss of C ions. Postfoil charge-state selection is used to measure the fixed-charge stopping cross sections for the fully stripped and one-electron C ions, and to extract the energy lost in the charge-change cycle $C^{6+} \rightleftarrows C^{5+}$ with the aid of a two-component charge-state model. The results show that charge-changing energy loss forms a significant part of the total stopping for 3-MeV/u C ions, and a significant higher-order Z_1-dependent effect is seen in the stopping cross section for C^{6+} ions. The standard interpretation in terms of the Bloch term and polarization theory is discussed in the light of these observations.

I. INTRODUCTION

A. Fast, light projectiles: Evolution of theory and experiment

The stopping power for fast, fully stripped projectiles (with velocity $v \gg 2Z_1e^2/\hbar$) is approximately described by Bethe's first-order quantal perturbation treatment[1] and is given by

$$\frac{dE}{dx} = \frac{4\pi e^4 N Z_2 Z_1^2}{mv^2} L_0(v,Z_2) , \tag{1}$$

where Z_1 and Z_2 are the atomic numbers, respectively, of the projectile and target, m and $-e$ are the mass and charge of the electron, N is the number of target atoms per unit volume, and v is the projectile velocity. The quantity L_0 is the well-known "stopping function."[2] The subject of higher-order Z_1-dependent corrections to this theory was born during the 1950s with the discovery by Barkas of a difference of several percent between the ranges of π^- and π^+ mesons in nuclear emulsion. This result conflicted with the obvious symmetry arising between the stopping of positive and negative particles in Bethe's treatment. The observation was supported by later, more precise measurements by Barkas *et al.*[3] In an attempt to improve on the theory, Ashley, Ritchie, and Brandt performed classical calculations of the response of distant target electrons to the projectile's potential, treating the electrons as bound in a harmonic-oscillator potential. The displacement of such an electron in its potential well was calculated in first order, leading to a Z_1^3-dependent polarization term in dE/dx with a magnitude dependent on the impact-parameter cutoff chosen against close collisions.[4] Similar calculations were presented soon afterwards by Jackson and McCarthy, using a cutoff at the quantal radius of the harmonic oscillator.[5] Subsequent calculations by Lindhard and Esbensen used an equivalent semiclassical approach in which the projectile was considered to interact with a free-electron gas.[2] Scattering of the target electrons is treated using a screened (Yukawa) potential, thereby enabling the potential of the induced electron cloud to be approximately incorporated.[6] These calculations resulted in a Z_1^3-dependent term nearly twice as large as Jackson and McCarthy's prediction, and in good agreement with experimental data on $\Sigma^{\pm}$ and $\pi^{\pm}$ ranges.[2,7] We should, however, note that the physical basis for the Lindhard-Esbensen model has recently been called into question. The polarization effect has been calculated[8] using a fully quantal treatment of the interaction between a bare projectile and an electron gas. The calculation suggests that the screened potential used in Ref. 2 is inappropriate for treating close collisions, and indicates that the polarization effect arising from close collisions is almost negligible. This result agrees with the assumptions of Refs. 4 and 5. However, an exact quantitative prediction for L_1 remains elusive.

A further higher-order correction to the Bethe theory was derived theoretically by Bloch[9,10] by considering the transition from the high-velocity Bethe regime to the low-velocity regime described by Bohr.[11] With the definition $\kappa = 2Z_1e^2/(\hbar v)$, this correction to the Bethe stopping function L_0 is given by

$$Z_1^2 L_2 = -\left[\frac{\kappa}{2}\right]^2 \sum_{n=1}^{\infty} \frac{1}{n[n^2+(\kappa/2)^2]} , \tag{2}$$

which for small Z_1 reduces to

$$Z_1^2 L_2 = -1.20\left[\frac{\kappa}{2}\right]^2 . \tag{3}$$

Since Eq. (2) is even in κ, the Bloch correction does not appear in comparisons between particles of opposite charge. However it is fundamentally important for predicting dE/dx for ions in matter, in particular the relationship between dE/dx values for light and heavy ions. Following Lindhard,[2] we express the overall effect of the polarization and Bloch corrections to the Bethe theory by the formula

$$L = L_0 + Z_1 L_1 + Z_1^2 L_2 \ . \tag{4}$$

Only one direct experimental test of Eq. (4) has been made using "random" targets. This was achieved through a series of experiments by Andersen *et al.*,[12,13] who studied the precise Z_1 dependence of dE/dx for fast light ions (with $Z_1 = 1,2,3$) in a range of targets (with $Z_2 \geq 13$). The technique of compensating calorimetry used in these experiments provided an opportunity for energy-loss measurements of almost unique precision, around 0.5% in the relative dE/dx for different ions in the same target. The measurements made with the three ions H, He, and Li were used to extract experimental values of L_0, L_1, and L_2 for comparison with the theoretical values. The results (Ref. 12) showed quite encouraging agreement with theory, using the value of L_1 calculated by Lindhard and Esbensen.

A closer fit to the data can be achieved by using the theory of Ashley, Ritchie, and Brandt for L_1, since the undetermined cutoff parameter b (of order unity) may be adjusted as an empirical parameter. This yields the value $b = 1.4$ for these data,[14] corresponding to a value of L_1 intermediate between the predictions of Refs. 5 and 2.

A more indirect method of testing Eq. (4), or specifically the polarization term L_1 in this equation, is to study the Z_2 dependence of stopping power for a given ion. This method is indirect because to obtain L_1, it is necessary to model the Z_2 dependence of the shell correction. The technique has been used in detailed studies of proton stopping in a wide range of random targets.[15] The data are fitted using adjustable parameters for the shell correction and L_1. A value of $b = 1.3$ is obtained from the fit.

For completeness, we also mention a detailed analysis by Bichsel and Porter[16] of published stopping-power data for H and He ions in low-Z gas targets. In this case, values of $b = 0.6$ in H_2 and He targets and $b = 1.8$ in N_2, O_2, and CH_4 were obtained. The significance of these variations is not clear. However, the polarization effect in such light targets is small, and some uncertainties may be associated with shell corrections and fluctuations in target-thickness measurements between different experiments. Overall, it appears that most of the available data[13,15] is consistent with a choice of $b \sim 1.4$.

B. Intermediate velocities: Physics problems and experimental techniques

As the projectile velocity is decreased, two things happen. First, the first-order quantal perturbation theory valid in the velocity region $v \gg 2Z_1 e^2/\hbar$ becomes increasingly inaccurate. This state of affairs is reflected by the presence of large higher-order correction terms as predicted by the theory described above. Second, the projectile stripping criterion $v \gg Z_1^{2/3} e^2/\hbar$, breaks down and projectile ions begin to capture electrons to bound states. This introduces energy losses occurring in charge-changing events, and it also means that projectile ions now have an effective charge which is determined by the number and screening effect of their bound electrons.

Faced with the complexity posed by simultaneous higher-order corrections and projectile effective charges, two approaches can be adopted in considering dE/dx for intermediate velocity ions. One may perform the most sophisticated available calculations of higher-order corrections and effective charges,[17] and compare these with the best measurements[18] of dE/dx over the largest possible range of ion and target species and ion velocity, in the hope of finding a satisfactory and predictive theory to describe all cases. Attempts in this direction have been made in recent years, but in a recent review[19] Andersen concluded that this kind of approach has revealed little about the basic physics behind dE/dx, and has not been especially successful in predicting dE/dx outside the range of pre-existing experimental data. In specific cases, some success has been achieved. Ritchie and Brandt[14] have analyzed data on the stopping of 2.0- and 3.5-MeV ions ($Z_1 = 1$–9) in Au,[20] where the high value of Z_2 leads to a large predicted Z_1^3-dependent term. Uncertainties in the effective charge of the ions are then relatively small and results consistent with the light-ion data ($b \simeq 1.4$) are obtained. Geissel *et al.*[21] have measured the stopping powers for 1.4-MeV/u heavy ions in Ar gas, a case for which the emergent charge-state distribution had previously been measured.[22] By introducing the observed mean charge state $\bar{q}$ into the theory in place of Z_1, Geissel *et al.* found agreement between their data and the prediction of Jackson and McCarthy,[4] and substantial disagreement with the prediction of Ref. 2. Nevertheless, such analyses depend fundamentally on assumptions which remain unverified; for example, it is almost universally assumed that the energy lost in charge-changing events is negligible except at very low energies.

As an alternative to making still further experiments on dE/dx for ions occupying a multiplicity of charge states, it is clearly desirable to use experimental techniques which break the complex dE/dx problem down into more accessible elements. An attractive way of doing this is to study the stopping cross sections for each projectile charge state in turn, so obtaining more direct experimental information on higher-order Z_1 effects as well as screening effects. This is the approach taken in the present work, and in a small number of previous experiments which we now briefly discuss.

C. Charge-state-specific stopping cross sections

To measure the stopping cross section for a specific projectile charge state, one needs to avoid charge-changing events. One way to achieve this is to perform energy-loss measurements with channeled ions, for which charge exchange is greatly reduced and it is possible to identify those ions which have traversed the channeling crystal

without charge exchange. An experiment designed to test for higher-order and screening effects in planar channeling was performed by Datz *et al.*[20] in 1977. Screening effects by bound projectile electrons were found to be almost complete, in agreement with the low-velocity model of Brandt,[17] and there appeared to be significant higher-order effects in the case of light ions. However, subsequent analysis showed that the apparent higher-order effects observed may have arisen from straggling effects on the shape of the energy-loss distribution.[23] For the heavier ions studied in that experiment, errors due to straggling were not significant and the stopping powers were found to be approximately proportional to Z_1^2.

In a later experiment,[24] Golovchenko *et al.* have measured the stopping power of the $\langle 110 \rangle$ axial channel in silicon for fully stripped 3.1-MeV/u ions in the atomic number range $Z_1=9-17$. They also observed stopping powers proportional to Z_1^2 to within their $\sim 1\%$ experimental precision. They subsequently argued that this apparent proportionality arises from a near cancellation between the Bloch term and the polarization term.[10] This could occur because the Bloch term in particular arises from close impact-parameter projectile-electron collisions, and is therefore substantially reduced in an axial channeling experiment. Nevertheless it is intriguing that, at least to the authors' knowledge, no channeling experiment has yet been reported which shows conclusive evidence of higher-order Z_1-dependent effects.

A second method by which charge-changing events can be avoided in dE/dx experiments is to use random targets which are thin compared with the mean free path for charge exchange. This type of experiment was first used by Allison and co-workers in early experiments with H and He ions at intermediate velocities $[v=(1.2-1.9) \times Z_1 e^2/h]$, using thin gas targets.[25,26] Their results show remarkably large deviations from Z_1^2 dependence of dE/dx for the fully stripped charge state of He, incomplete screening for partially stripped ions, and a large contribution to thick-target dE/dx arising from individual charge-changing events. Unfortunately this painstaking work appeared long before higher-order corrections to dE/dx became generally accepted, and has only rarely been quoted in the literature.

Our present experiment uses this same concept, although the experimental technique is considerably different. Our objective is to extend present knowledge of higher-order Z_1-dependent effects away from the lightest ion species, towards the heavy-ion region. This paper reports a first step in this direction, which already raises some significant questions about the role of charge-changing energy losses in dE/dx for heavy ions. The principle of our technique is to use target foils so thin that the probability of charge exchange is reduced to a few percent. Residual charge-changing effects are minimized by charge-state selection of the emergent ions, using a magnetic spectrometer. In addition to thin-target measurements, thicker targets are also used to study the onset of charge-changing processes and their effect on dE/dx. Two averaging systems are employed which allow measurements of fractional energy losses of $\sim 10^{-4}$ to be made to a precision of 1%.

II. EXPERIMENT

A. Basic requirements for precision measurement

The systems chosen for study are 3-MeV/u He, Li, and C ions incident on thin C foils. Both He and Li ions are essentially fully stripped of their electrons at this velocity, but C ions possess a significant one-electron fraction ($\sim 18\%$).[27] To study higher-order Z_1-dependent effects for fully stripped He, Li, and C projectiles, and the stopping for the one-electron C projectile, we require foil thicknesses ranging down to about 2 μg/cm^2. This thickness is small enough to permit almost complete charge-state selectivity in the energy-loss measurement for C ions. Carbon is chosen as the target material because it can be manufactured as a self-supporting foil several mm across, even at 2 μg/cm^2 thickness.

The energy loss for He in the thinnest foils is around 10^{-4} of the incident energy, and to obtain useful experimental observations on higher-order Z_1 effects we require an experimental precision of $\sim 1\%$. Our experiment is therefore designed with a view to making energy-loss measurements to a precision of about 10^{-6} of the incident beam energy. To allow direct detection of the beam with solid-state detectors the beam intensity is reduced to about 10^3 counts s^{-1}. The total beam fluence on a foil throughout the entire experiment is then around 10^7 cm^{-2} which has the advantage that carbon buildup is reduced to negligible levels. With an instrumental response function whose standard deviation is σ, the statistical error in an energy measurement after detecting N particles is $\sigma/\sqrt{N}$. Detector damage considerations limit the beam fluence on the detector to around 10^7 particles, and we employ $\sim 10^2$ foil changes per beam species during the experiment, so limiting N to around 10^5. Consequently our precision criterion leads us to the requirement $\sigma/T < 3\times 10^{-4}$ where T is the incident beam energy, or $\sigma < 1$ keV/u. This criterion is barely met by the theoretical resolution limit for solid-state detectors.[28] Since post-foil charge-state selection is required in any case to minimize residual charge-changing effects in the thin C foils, it is convenient to use a magnet-spectrometer—position-sensitive-detector (PSD) system to provide both charge-state selection and improved energy resolution. With this system, the PSD position signal is passed in the usual way to an analog-to-digital converter—multichannel-analyzer and the foil-in, foil-out results stored as separate spectra with centroid channels $\bar{X}_{\text{in}}$ and $\bar{X}_{\text{out}}$. The magnet equation then determines the energy loss E as

$$\frac{E}{T}=(\bar{X}_{\text{out}}-\bar{X}_{\text{in}})\frac{df}{d\chi}\frac{2}{f}+O((E/T)^2)\ , \tag{5}$$

where f is the magnetometer frequency. The second-order term is negligible because of the small value of E/T.

A number of sources of systematic error exist in this kind of experiment. One important class of errors arises because the energy loss is determined from the difference of two similar energies. Errors can arise from time-dependent variations in any of the quantities shown in Eq. (5), since an inevitable time delay occurs between measure-

ments with foil in and foil out of the beam. In particular, beam energy fluctuations on a Tandem accelerator are likely to occur at the level of $10^{-5}T$, on a variety of time scales. Magnet power supplies have similar limitations. Rather than isolating every significant source of time-dependent fluctuation and minimizing it, an averaging system can be employed to smooth out any fluctuations. This approach is adopted for the present experiment, and proves to be highly successful.

A second class of systematic errors arises from the calibration factor $df/d\chi$ in Eq. (5). Various sources of differential nonlinearity, notably the PSD position response, can create difficulties in determining the correct value for $df/d\chi$. Once again an averaging procedure is required to smooth out nonlinearities by making a number of energy-loss measurements along the length of the PSD.

Systematic errors can also occur as a result of beam scattering from the edge of foil holders. This scattering is only present when a foil is in position and would therefore enhance the apparent energy loss in the foil when the peak centroids are measured. The geometry of the experiment and the data-collection system therefore have to be controlled so that this type of error is ruled out.

Because of the single focusing nature of the Buechner spectrometer[29] used in this work (focusing in the dispersive plane only) a further possible scattering related source of error must be considered. In the case of single collisions the correlation between electronic energy transfer (e.g., inner-shell ionization events) and angle of scatter could lead to systematic errors if part of the distribution is cut off. To eliminate this possibility the angular spread of the energy-loss distribution in the nondispersive plane is monitored to ensure it falls within the PSD acceptance angle.

Finally, a subtle error can occur as a result of spectrometer aberrations. The beam with foil out enters the spectrometer as a fine pencil, whereas the beam after passage through a thin foil has a very small divergence angle of $\sim$mrad. The magnet deflects the two beams differently owing to a slight variation in the effective magnet radius at different scattering angles. The magnitude of this error is estimated for our Buechner spectrometer to be $<10^{-6}T$ for a 3-MeV/u He, Li, or C ion in a 2-μg/cm^2 C foil. Rather than attempt such a small correction to our data, we shall neglect the effect. Since the spectrometer is operated at its minimum aberration position,[24] all other aberrations are negligible.

B. Experimental systems

A schematic of the physical layout is shown in Fig. 1. The beam emerges from the analyzing magnet of the 6.5-MV Harwell Tandem, which is stabilized by a generating voltmeter system in order to permit transmission of low-intensity beams ($\sim$nA). The beam passes through two small collimators A and B, partly to attenuate the beam to an intensity of $\sim 10^3$ counts sec^{-1}, and partly to provide the fine pencil beam necessary for optimum energy resolution in the spectrometer. Collimator B is placed about 4 mm upstream from the foil position, located at the object plane of the spectrometer. The beam then

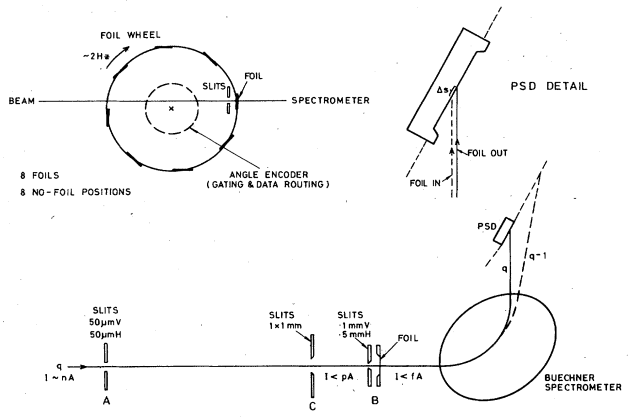

FIG. 1. Schematic of the experimental layout. Insets show detail of the rotating foil wheel and the focal plane position sensitive detector.

enters the spectrometer at 0°, and is detected in the image plane by a 15-mm-long PSD with position resolution of ~ 100 μm.

The time-averaging system consists of a rotating target wheel with eight target positions, driven by a dc motor. The angular position of the wheel is measured by an optical shaft encoder with an angular resolution of 1600 units per revolution, and the output is used to gate the signals from the PSD and route them into 16 separate datasets corresponding to the 8 foil positions and 8 intermediate foil-out positions. Because a dc motor is used the rotation speed is decoupled from time-varying quantities such as the accelerator's terminal potential or the analyzing magnet field, thereby avoiding correlation effects. To obtain a reasonable average over time the wheel is run at speeds of around 120 rpm. Thus 80 min data-collection time is sufficient to perform essentially 10^4 successive measurements.

A second averaging system deals with differential nonlinearity in the response of the PSD and associated electronics. This nonlinearity can be a particular problem in the Buechner spectrometer; in the Harwell instrument the beam is incident at 70° to the normal of the focal plane. This magnifies the effect of any undulation in the PSD front surface and may produce significant problems even with an apparently planar detector. The averaging system deals with the problem by stepping the spectrometer magnetic field and collecting data at up to 64 separate positions along the length of the detector. The system operates automatically, dumping the data collected at each detector position (eight foil-in and eight foil-out spectra) on line to a VAX computer before initiating the next data-collection step. The computer is subsequently used to combine the data into a single spectrum for each foil-in and foil-out position. The field-stepping system is also a convenient means of performing the detector calibration required to evaluate Eq. (5).

C. Experimental operation

Collimators A, B, and C are optically aligned to the beam-line axis with the spectrometer set at 0°. Collima-

tors A and B are then withdrawn and the beam path is steered as necessary to optimize the current in a Faraday cup located downstream from the target position. This beam path is constrained by collimator C. Collimators A and B are then placed on axis. The beam intensity through A is reduced by adjusting accelerator parameters, and is monitored by a scintillator placed a few cm downstream from A. A surface-barrier detector downstream of the target position is used to monitor the final beam intensity before exposing the detectors in the spectrometer.

In addition to PSD $P1$ which is used to measure energy loss a second PSD $P2$ is mounted in the spectrometer focal plane, perpendicular to the dispersion direction, to check the central position of $P1$ relative to the beam plane. This check is performed each time a beam is set up, and if necessary the lateral position of $P1$ and $P2$ is slightly adjusted. $P2$ is also used to observe the scattering width of the beam from each target. This information is used to confirm calculations that the proportion of beam scattered beyond the sides of $P1$ during an energy-loss measurement is negligible.

To perform a full energy-loss measurement, the foil wheel is set in motion and the routing system used to collect 16 256-channel spectra on a 4096-channel analyzer. Each 256-channel spectrum corresponds to the spectrum from a foil-in or foil-out position. The spectrometer field is cycled and then set to position the beam on the PSD, about 10% of the PSD length away from one end. Data is collected for a fixed number of counts before the field is automatically stepped and the data dumped on-line to the computer. Following a preset time delay of about 40 sec for the magnetic field to stabilize, the next data-acquisition period is started. An energy-loss measurement typically comprises 64 such steps along the length of the detector.

The PSD calibration is carried out in a similar manner. Typically only nine steps are used, to minimize any drift in the beam energy which is assumed constant for calibration purposes. Since such drifts could be a significant source of error, calibrations are repeated to check reproducibility, and are not always performed in the same direction along the detector. With care, calibration errors are reduced to the level of $\sim 0.7\%$.

D. Data reduction

For each foil-in and foil-out position (16 in all) a complete energy-loss measurement for a given ion species involves 64 data sets taken along the length of the PSD. The peak position for each of these data sets is found, using a computer program for ease of analysis. To minimize the influence of the "tail" of the spectrum arising from slit-scattered beam, the program then takes the centroid of a region extending several standard deviations either side of the peak position. Since the slit scattering is present in both foil-in and foil-out spectra, its effect on the centroid cancels when the difference $\bar{X}_{\text{out}} - \bar{X}_{\text{in}}$ is calculated. (Nevertheless, care is taken in the experiment to minimize slit scattering as it can introduce significant statistical errors in the results.) The width of the region chosen for calculating the centroid is also varied to check for any systematic effects. The eight foil-out centroids are averaged to obtain a best estimate for the foil-out centroid corresponding to each beam position on the PSD.

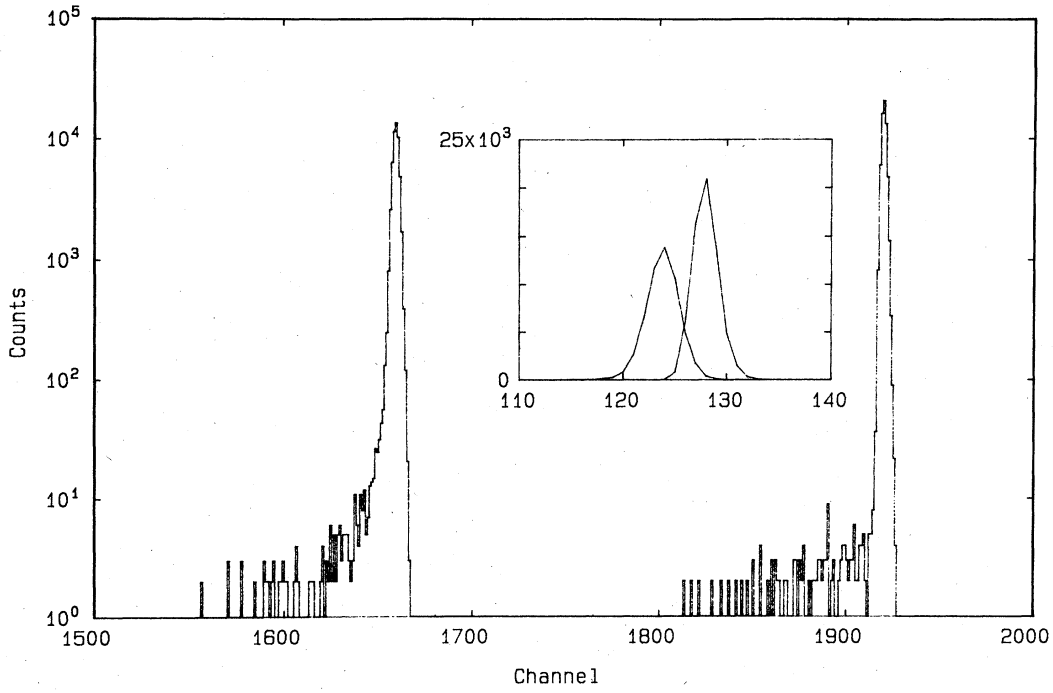

FIG. 2. Summed spectra for foil in and foil out as described in text. As expected both peaks exhibit the same low slit-scattering background. Foil-in spectrum (3-MeV/u C in a 7.5-μg cm^{-2} C foil) exhibits skewing characteristic of thin-foil energy loss. Inset linear plot is an overlay of the two spectra illustrating the channel shift for this foil.

The 64 separate data sets can now be combined into one spectrum for each foil-in—foil-out position. This is done by shifting each spectrum by the number of channels corresponding to the foil-out centroid, and summing the resulting spectra. The result is illustrated in Fig. 2 which shows an example of two summed spectra, foil in and foil out.

The calibration of PSD channel number against magnotometer frequency is computed using spectrum data sets obtained in a sequence of nine steps along the PSD. The peak centroids $\bar{\chi}_i$ are calculated as above, and the calibration curve generated as a sequence of eight straight-line segments connecting the points (f_i,χ_i) with slope $(d\chi/df)_i=(\chi_i-\chi_{i-1})/(f_i-f_{i-1})$. To convert a given channel shift $(\bar{\chi}_{\text{out}}-\bar{\chi}_{\text{in}})$ obtained in an energy-loss measurement into the required energy loss E using Eq. (5), the appropriate calibration segment is chosen according to the value of $\chi_m=(\bar{\chi}_{\text{out}}+\bar{\chi}_{\text{in}})/2$. If χ_m falls outside the calibration region, the data is rejected. This procedure is followed for each energy-loss measurement along the PSD, and the resulting values of ΔE are averaged to obtain the final estimate of E for each foil. The output also includes a value of E for each of the eight foil-out positions, as a check on the time-averaging system. If this system is operating successfully, these E values should naturally be zero to within the calculated statistical precision. This has always been found to be the case in the present experiment.

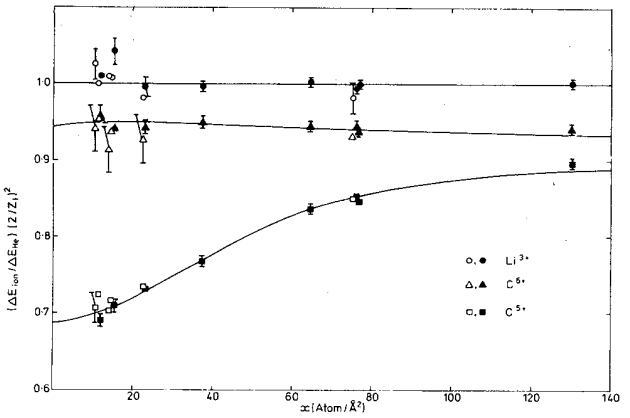

FIG. 3. Reduced energy losses for 3-MeV/u Li and C ions, relative to measured He energy losses at the same velocity. Departures from unity indicate deviations from Z_1^2 scaling in dE/dx. In the case of carbon 5+ and 6+ the nonequilibrium nature of the charge-state distribution is evident. Solid curves represent least-squares fits to the C^{5+} and C^{6+} data. From this we extract the stopping cross sections for the fixed charge states 5+ and 6+, and the energy loss in charge-changing events. (ΔE is denoted E in the text.)

III. RESULTS AND DISCUSSION

A. Projectile-charge dependence of dE/dx

In order to examine any departures from Z_1^2 scaling of dE/dx in our data, it is useful to present the energy-loss result in the reduced form $(E_{\text{ion}}/E_{\text{He}})(2/Z_1)^2$, as shown in Fig. 3. The He data are chosen for normalization purposes because for 3-MeV/u He ions, higher-order Z_1-dependent effects predicted by theory are small, and the ions are essentially fully stripped of electrons. The foil thicknesses used in the abscissa are estimates derived from the He energy-loss data, using the stopping power compilation of Ziegler.[30] The relative precision of our energy-loss data is indicated by the error bars in Fig. 3.

The Li results are seen to scale approximately as Z_1^2 relative to the He data. This is consistent with the standard theoretical prediction based on the Bloch correction plus a polarization term, as shown in Table I. However, the data for both C^{6+} and C^{5+} ions show strong departures from Z_1^2 scaling. Three basic features appear.

(1) The data for the two charge states converge as the foil thickness increases. This is a novel effect in an experiment measuring energy loss in solids. The broad trend of convergence may be understood in qualitative terms, as the result of charge-state equilibration within the target.

(2) The data for C^{6+} and C^{5+} ions in thin foils, in which charge exchange is suppressed, are significantly lower than the scaled He value.

(3) The convergence towards an equilibrium stopping power appears much more strongly in the 5+ than in the 6+ data.

As will become apparent, features (2) and (3) of the data are of fundamental importance.

To interpret the data in full, it is necessary to take into account the processes of electron capture and loss which the C projectile may undergo as it passes through a foil. Recently, experimental data on charge-changing cross sections for 3-MeV/u C ions in C targets have been report-

TABLE I. Theoretical higher-order corrections for 3 MeV/u He, Li, and C^{6+} ions in C targets, compared with our experimental observations. Columns 2 and 3: polarization term. Column 4: Bloch term. Columns 5 and 6: sum of polarization and Bloch terms, giving the theoretical higher-order correction. Columns 7 and 8: theoretical higher-order correction relative to He. Column 9: observed higher-order effect relative to He.

	Z_1L_1/L_0 (%)			Δ_{ion} (%)		$(\Delta_{\text{ion}}-\Delta_{\text{He}})/L_0$ (%)		
Ion	Jackson and McCarthy (A)	Lindhard and Esbensen (B)	$Z_1^2L_2/L_0$ (%)	Theory A	Theory B	Theory A	Theory B	Exp.
He	0.9	1.8	−0.9	0	0.9			
Li	1.4	2.7	−1.9	−0.5	0.8	−0.5	−0.1	0±1
C^{6+}	2.7	5.4	−6.5	−3.8	−1.1	−3.8	−2.0	−2.8±0.7

ed.[27] At this energy the charge states 5+ and 6+ are found to account for over 98% of the charge-state distribution at equilibrium, and the electron loss and capture cross sections in typical evaporated C foils are found to be $\sigma_{10}=0.052$ Å^2/atom and $\sigma_{01}=0.0102$ Å^2/atom. These cross sections describe the evolution of the observed 5+ and 6+ charge fractions as a function of target thickness, via the usual two-component charge-state model.[31] Since for such highly stripped ions post-foil Auger processes can be neglected, one may reasonably claim that the observed charge-state distribution truly reflects the degree of projectile ionization within the target foil. The stopping power should then vary as a function of the charge-state distribution as this evolves with foil thickness, as determined by the cross sections σ_{01} and σ_{10}.

B. Charge-exchange model for energy loss

A useful transport formalism for evaluating moments of the energy-loss distribution in thin targets on the basis of charge-changing cross sections has been described by Winterbon.[32] We adopt this formalism with the simplifying assumption that the slowing down in a given charge state is continuous. This assumption is good for present purposes because we are not concerned with energy straggling. Consider the probability distribution $f_i(x,E)$ for an ion to have lost energy E and to be in charge state i, having traveled distance x through a target. Let the energy loss in the charge-change $i\rightarrow j$ have a mean value $\bar{\epsilon}_{ij}$, and let us neglect the distribution about $\bar{\epsilon}_{ij}$. Furthermore, let the stopping cross section for ions which do *not* change their charge be given by S_{ii}, where the second subscript indicates that the charge remains fixed. Then the evolution of f_i as a function of x is given by the set of i partial differential equations

$$\frac{\partial f_i}{\partial x}+S_{ii}\frac{\partial f_i}{\partial E}\sum_{j\neq i}[\sigma_{ji}f_i(x,E-\bar{\epsilon}_{ji})-\sigma_{ij}f_i(x,E)]\ . \quad (6)$$

This set is conveniently solved in terms of the nth energy moment for charge state i at depth x,

$$g_i(x,n)=\int_0^\infty dE\,E^n f_i(x,E)\ . \quad (7)$$

From this definition the charge-state fraction at depth x is

$$\phi_i(x)=g_i(x,0)\ , \quad (8)$$

and the mean energy loss for charge state i at depth x is

$$\bar{E}_i=g_i(x,1)/g_i(x,0)\ . \quad (9)$$

Expanding $f_i(x,E-\bar{\epsilon}_{ji})$ as a Taylor series about E, and taking first moments of Eqs. (6), yields the exact result

$$\frac{dg_i(x,1)}{dx}=S_{ii}g_i(x,0)+\sum_{j\neq i}\{\sigma_{ji}[g_j(x,1)+\bar{\epsilon}_{ji}g_j(x,0)]-\sigma_{ij}g_i(x,1)\}\ . \quad (10)$$

For two charge states only, using the more familiar notation of ϕ_i and $\bar{E}_i$ [Eqs. (8) and (9)], this reduces to the two simultaneous equations

$$\frac{d}{dx}(\phi_a\bar{E}_a)=S_{aa}\phi_a+\sigma_{ba}\phi_b(\bar{E}_b+\bar{\epsilon}_{ba})-\sigma_{ab}\phi_a\bar{E}_a\ , \quad (11)$$

$$\frac{d}{dx}(\phi_b\bar{E}_b)=S_{bb}\phi_b+\sigma_{ab}\phi_a(\bar{E}_a+\bar{\epsilon}_{ab})-\sigma_{ba}\phi_b\bar{E}_b\ . \quad (12)$$

Defining a as the incident charge state, we have the initial conditions

$$\phi_a(0)=1,\ \ \phi_b(0)=0 \quad (13)$$

as well as

$$\bar{E}_a(0)=0,\ \ \bar{E}_b(0)=0. \quad (14)$$

Summing Eqs. (11) and (12) and solving the resulting differential equation leads to the result

$$\phi_a\bar{E}_a+\phi_b\bar{E}_b=[(S_{aa}+\sigma_{ab}\bar{\epsilon}_{ab})(\sigma_{ba}x+\phi_b)+(S_{bb}+\sigma_{ba}\bar{\epsilon}_{ba})(\sigma_{ab}x-\phi_a)]/\alpha\ , \quad (15)$$

where $\alpha=\sigma_{10}+\sigma_{01}$, and

$$\phi_a=(\sigma_{ba}+\sigma_{ab}e^{-\alpha x})/\alpha\ . \quad (16)$$

Equation (15) can now be used to decouple Eqs. (11) and (12), so obtaining

$$\left[\frac{d}{dx}+\alpha\right](\phi_a\bar{E}_a)=A+Bx+Ce^{-\alpha x}\ , \quad (17)$$

where

$$A=S_{aa}-C\ , \quad (18)$$

$$B=\frac{\sigma_{ba}}{\alpha}(S_{aa}\sigma_{ba}+S_{bb}\sigma_{ab}+U\sigma_{ab}\sigma_{ba})\ , \quad (19)$$

$$C=\frac{\sigma_{ab}}{\alpha^2}(S_{aa}\sigma_{ab}+S_{bb}\sigma_{ba}-U\sigma_{ab}\sigma_{ba})\ , \quad (20)$$

and $U=\bar{\epsilon}_{ab}+\bar{\epsilon}_{ba}$.

The solution to Eq. (17) with the initial conditions (13) and (14) is finally

$$\phi_a\bar{E}_a=\frac{B}{\alpha}x+\frac{1}{\alpha}\left[A-\frac{B}{\alpha}\right](1-e^{\alpha x})+Cxe^{-\alpha x}\ . \quad (21)$$

This expresses the mean energy loss $\bar{E}_a$ for ions at depth x with the same charge state as the incident beam, precisely the quantity measured in the present experiment. The solid curves shown in Fig. 3 are the result of fitting Eq. (21) to our energy-loss data for 6+ (zero-electron) and 5+ (one-electron) C ions, with the quantities S_{00}, S_{11}, and $U=\bar{\epsilon}_{01}+\bar{\epsilon}_{10}$ left as free parameters in the fit. The quality of the fit ($\chi^2=0.6$) suggests that the measured charge-changing cross sections do appropriately describe the evolution of projectile ionization within the foil. Independent evidence for this conclusion is also found in the excited-state population studies of Woods.[27] The fixed-charge stopping cross sections S_{00} and S_{11} relative to the He stopping cross section are given by the $x=0$ intercepts of the solid-line fits in Fig. 3. The fitted value of U is 2.3 ± 0.22 keV. If U is set to zero in the fitting procedure

and only S_0 and S_1 are allowed to be adjusted, the value of χ^2 increases by a factor of 5.

C. Comparison of observed stopping parameters with theory

The basis from which higher-order corrections in stopping theory have been developed is Bethe's first-order quantal perturbation theory.[1] In that treatment the ion is considered as a time-dependent perturbing potential, and the essence of the theory lies in evaluating the generalized oscillator strength connecting initial and final states of the target system.[33] To provide some continued basis for testing higher-order corrections in partially stripped systems (e.g., our present case of 3-MeV/u C ions in C targets), the Bethe theory must be "stretched" in some way to account for the presence of charge-changing events. This is true even when one deals only with the fully stripped charge state within the charge-state distribution. For example, the total stopping cross section for the fully stripped C ion may be written as

$$S_0 = S_{00} + S_{01} = S_{00} + \bar{\epsilon}_{01}\sigma_{01} , \tag{22}$$

where S_{01} is the contribution arising from electron capture from the target system to the projectile. We must decide whether S_0 or S_{00} is the more appropriate quantity to associate with the Bethe theory. In our present discussion we choose S_0, thereby including electron transfer to the projectile simply as another form of target ionization.

Approximate theoretical estimates for the quantities $\bar{\epsilon}_{01}$ and $\bar{\epsilon}_{10}$ which make up our measured parameter U can be attempted as follows. We adopt the convention of accounting only the *kinetic* energy of the projectile *nucleus* when calculating the energy lost by the projectile: The temporary binding and kinetic energy associated with a projectile's bound electron is not included. Since velocity matching ensures that $K \rightarrow K$ shell transfer is the major electron capture channel in the 3-MeV/u C on C system, we assume for present purposes a target atom ionization potential of 284 eV (the C K-shell binding energy). The kinetic energy given to the captured electron by the linear motion of the projectile constitutes a further energy loss of 1.63 keV. Hence we obtain $\bar{\epsilon}_{01} = 1.91$ keV. Regarding electron loss from the projectile, we estimate $\bar{\epsilon}_{10}$ from the effective continuum level to which the projectile's bound electron is raised, following the approach of Janev and Presnyakov.[34] This procedure yields a value for the 3-MeV/u C on C system of $\bar{\epsilon}_{10} = 0.3$ keV. From these results we obtain $U = \bar{\epsilon}_{01} + \bar{\epsilon}_{10} = 2.2$ keV, in good agreement with our experimental result of (2.3 ± 0.2) keV. However, we should note that, since our two-component charge-state model neglects the small ($< 2\%$) fraction of C^{4+} ions at equilibrium, our experimental value of U could be too low by an amount < 0.5 keV. Thus our estimate of charge-changing energy losses is somewhat conservative.

Having obtained estimates for S_{00}, S_{11}, $\bar{\epsilon}_{01}$, and $\bar{\epsilon}_{10}$ we are now in a position to calculate the total stopping cross sections for the fully stripped and one-electron charge states, S_0 and S_1.

1. *Fully stripped C ions*

We express the higher-order effect for a given fully stripped ion as $\Delta_{\text{ion}} = (L_{\text{ion}} - L_0)/L_0$. Thus the higher-order effect relative to He ions will be given by $(\Delta_{\text{ion}} - \Delta_{\text{He}})$ to sufficient precision for present purposes. Including a generous 20% uncertainty in the value of $\bar{\epsilon}_{01}$, Eq. (22) leads us to the result $(S_0/S_{\text{He}})(Z_{\text{He}}/Z_{\text{C}})^2 = 0.972 \pm 0.007$, or in difference terms $\Delta_{\text{ion}} - \Delta_{\text{He}} = (2.8 \pm 0.7)\%$. Table I compares this experimental result with standard theoretical predictions based on the Bloch term plus a polarization term. The observed higher-order effect lies between the values obtained by using the polarization theories of Jackson and McCarthy,[4] and Lindhard and Esbensen[5] and is roughly consistent with the value $b = 1.4$ in the theory of Ashley, Ritchie, and Brandt. We comment on the validity of the available theory in Sec. III D.

2. *One-electron C ions*

For the one-electron ion, the total stopping cross section is estimated from

$$S_1 = S_{11} + \bar{\epsilon}_{10}\sigma_{10} , \tag{23}$$

where the contribution of electron capture events to form the He-like C ion is neglected. This yields the numerical result $(S_1/S_{\text{He}})(Z_{\text{He}}/Z_{\text{C}})^2 = (0.703 \pm 0.007)$. This quantity is not easily related to standard stopping theory for two reasons. First, at least part of $\bar{\epsilon}_{10}$ arises from *projectile* ionization, not considered in standard stopping theory. Second, the effective charges appropriate to the first-order (Bethe) and polarization terms will be different from the charge ($\sim Z_1$) appropriate to the Bloch term. This is because the Bloch term is associated only with close impact-parameter projectile-electron collisions. In view of this complexity we await further data to be obtained using heavier ions before attempting any detailed analysis for the one-electron ion. It is however worth noting that the screening of the projectile charge by its single bound electron appears to be nearly complete as regards the dominant first-order stopping term.

D. Higher-order effects due to polarization and electron capture

The present results for S_0, the total stopping cross section for the fully stripped ion, are consistent with previous data on S_0 obtained with H, He, and Li ions.[13] All of these data are described, at least in a phenomenological way, by Eq. (4) with L_1 as given by the theory of Ref. 4 with $b \simeq 1.4$. In the absence of further information, this would have appeared to provide continued support for a straightforward polarization model coupled with the Bethe-Bloch stopping power.

It is here that the more microscopic approach taken in the present study is useful. We observe that energy losses associated with charge-changing events contribute to the stopping cross section a term of similar magnitude to the theoretical polarization term. This immediately casts doubts on the general validity of Eq. (4) in describing even

the stopping cross section for bare incident ions, S_0. Polarization effects cannot be the whole story.

We may formally include charge-changing effects by writing (for the bare-ion example)

$$L = L_0 + Z_1 L_1 + Z_1^2 L_2 + L_3(Z_1, Z_2, v) .$$

The new term L_3 represents a higher-order correction associated with electron transfer to bound states of the one-electron ion.

Since electron transfer cross sections display a highly complex behavior as a function of Z_1, Z_2, and v, L_3 is likely to be correspondingly complex. For light ions (H, He, Li) at MeV/u energies, L_3 is probably negligible at least in heavy targets. However, for heavier ions at MeV/u energies, L_3 may become significant. For example, the present experiment which makes an initial step towards the heavy-ion regime, shows that about 2% of the energy loss for 3-MeV/u C ions in C arises from charge-changing events. This proportion is likely to increase for ions heavier than C, and the term L_3 may ultimately exceed the polarization term. We expect further experimental studies on charge-state-specific stopping powers for heavy ions will prove fruitful.

IV. CONCLUSIONS

In order to describe the stopping power for partially stripped heavy ions in matter the energy loss involved in charge-changing collisions has to be accounted for in a manner similar to that first suggested by Allison *et al.*[25,26] This point is likely to become of major importance for very heavy ions. In our case of 3-MeV/u C ions the observed energy loss in these collisions agrees with straightforward theoretical estimates. In addition we observe departures from Z_1^2 dependence of dE/dx which are numerically consistent with the Bloch Z_1^4 term plus a polarization term as given by Ref. 4 with $b \simeq 1.4$ (i.e., intermediate between the predictions of Refs. 5 and 2). However, we emphasize that a direct comparison with these theoretical terms is unrealistic, in view of the presence of electron capture processes. Clearly further theoretical work with specific inclusion of charge-exchange processes is desirable to help clarify this situation more generally. Finally, we confirm the existence of pre-equilibrium energy-loss behavior associated with the statistical approach of the beam towards charge-state equilibrium within the solid target.

ACKNOWLEDGMENTS

It is a pleasure to acknowledge the generous assistance of D. J. Parker and J. Asher in developing the data-acquisition system, and M. Miller in providing thin high-quality carbon foils. We are also grateful to H. H. Andersen, P. T. Greenland, and J. M. Freeman for valuable discussions. L.B.B. acknowledges travel support from a NATO grant.

*Present address: JET (Joint European Torus) Joint Undertaking, Abingdon, Oxon OX14 3EA, United Kingdom.

†Permanent address: College of Health and Applied Science, Southwest Missouri State University, Springfield, Missouri, 65802.

[1]H. A. Bethe, Ann. Phys. (Leipzig) **5**, 325 (1930).

[2]J. Lindhard, Nucl. Instrum. Methods **132**, 1 (1976); H. Esbensen, Ph.D. Thesis, Aarhus University, Denmark, 1977 (unpublished).

[3]W. H. Barkas, N. J. Dyer, and H. H. Heckman, Phys. Rev. Lett. **11**, 26 (1963).

[4]J. C. Ashley, R. H. Ritchie, and W. Brandt, Phys. Rev. B **5**, 2393 (1972); Phys. Rev. A **8**, 2402 (1972).

[5]J. D. Jackson and R. L. McCarthy, Phys. Rev. B **6**, 4131 (1972).

[6]J. Lindhard, K. Dan. Vidensk. Selsk. Mat.-Fys. Medd. **28**, No. 8 (1954).

[7]H. H. Heckman and P. J. Lindstrom, Phys. Rev. Lett. **22**, 871 (1969).

[8]C. C. Sung and R. H. Ritchie, Phys. Rev. A **28**, 674 (1983).

[9]F. Bloch, Ann. Phys. (Leipzig) **16**, 285 (1933).

[10]J. A. Golovchenko, D. E. Cox, and A. N. Goland, Phys. Rev. B **26**, 2335 (1982).

[11]N. Bohr, K. Dan. Vidensk. Selsk. Mat.-Fys. Medd. **18**, No. 8 (1948).

[12]H. H. Andersen, H. Simonsen, and H. Sorensen, Nucl. Phys. **A125**, 171 (1969).

[13]H. H. Andersen, J. F. Bak, H. Knudsen, P. Møller Petersen, and B. R. Nielsen, Nucl. Instrum. Methods **140**, 537 (1977); H. H. Andersen, J. F. Bak, H. Knudsen, and B. R. Nielsen, Phys. Rev. A **16**, 1929 (1977).

[14]R. H. Ritchie and W. Brandt, Phys. Rev. A **17**, 2102 (1978).

[15]R. Ishiwari, N. Shiomi, and N. Sakamoto, Nucl. Instrum. Methods **194**, 61 (1982).

[16]H. Bichsel and L. E. Porter, Phys. Rev. A **25**, 2499 (1982).

[17]W. Brandt and M. Kitagawa, Phys. Rev. B **25**, 5631 (1982).

[18]For example H. Geissel, Y. Laichter, W. F. W. Schneider, and P. Armbruster, Nucl. Instrum. Methods **194**, 21 (1982); J. M. Anthony and W. A. Lanford, Phys. Rev. A **25**, 1868 (1982).

[19]H. H. Andersen, Phys. Scr. **28**, 268 (1983).

[20]S. Datz, J. Gomez del Campo, P. F. Dittner, P. D. Miller, and J. A. Biggerstaff, Phys. Rev. Lett. **38**, 1145 (1977).

[21]H. Geissel, Y. Laichter, W. F. W. Schneider, and P. Armbruster, Phys. Lett. **99A**, 77 (1983).

[22]W. Erb, Dissertation, 1978 [Gesellschaft für Schwerionenforschung (Darmstadt) Bericht P-7-78].

[23]S. P. Ahlen, Phys. Rev. Lett. **39**, 1398 (1977).

[24]J. A. Golovchenko, A. N. Goland, J. S. Rosner, C. E. Thorn, H. E. Wegner, H. Knudsen, and C. D. Moak, Phys. Rev. B **23**, 957 (1981).

[25]S. K. Allison, J. Cuevas, and M. Garcia-Munoz, Phys. Rev. **127**, 799 (1962).

[26]J. Cuevas, M. Garcia-Munoz, P. Torres, and S. K. Allison, Phys. Rev. **135**, A335 (1964).

[27]C. J. Woods, C. J. Sofield, N. E. B. Cowern, M. Murrell, and J. Draper, J. Phys. B **17**, 867 (1984); C. J. Woods, D. Phil. thesis, Oxford, U.K. (1983).

[28]J. B. A. England, *Techniques in Nuclear Structure Physics* (Macmillan, London, 1974), Pt. 1.

[29]C. P. Browne and W. W. Buechner, Rev. Sci. Instrum. **27**, 899

(1956).
[30]J. F. Ziegler, *The Stopping and Ranges of Ions in Matter* (Pergamon, New York, 1981), Vol. 5.
[31]S. K. Allison, Rev. Mod. Phys. **30**, 1137 (1958).
[32]K. B. Winterbon, Nucl. Instrum. Methods **144**, 311 (1977).
[33]M. Inokuti, Rev. Mod. Phys. **43**, 297 (1971).
[34]R. K. Janev and L. P. Presnyakov, J. Phys. B **13**, 4233 (1980).